Supplementary Materials for

Brief Communication: Effects of different saturation vapor pressure calculations on simulated surface-subsurface hydrothermal regimes at a permafrost field site

Xiang Huang, Charles J. Abolt, and Katrina E. Bennett

Earth and Environmental Sciences, Los Alamos National Laboratory, Los Alamos, NM, 87545 USA

Contents of this file

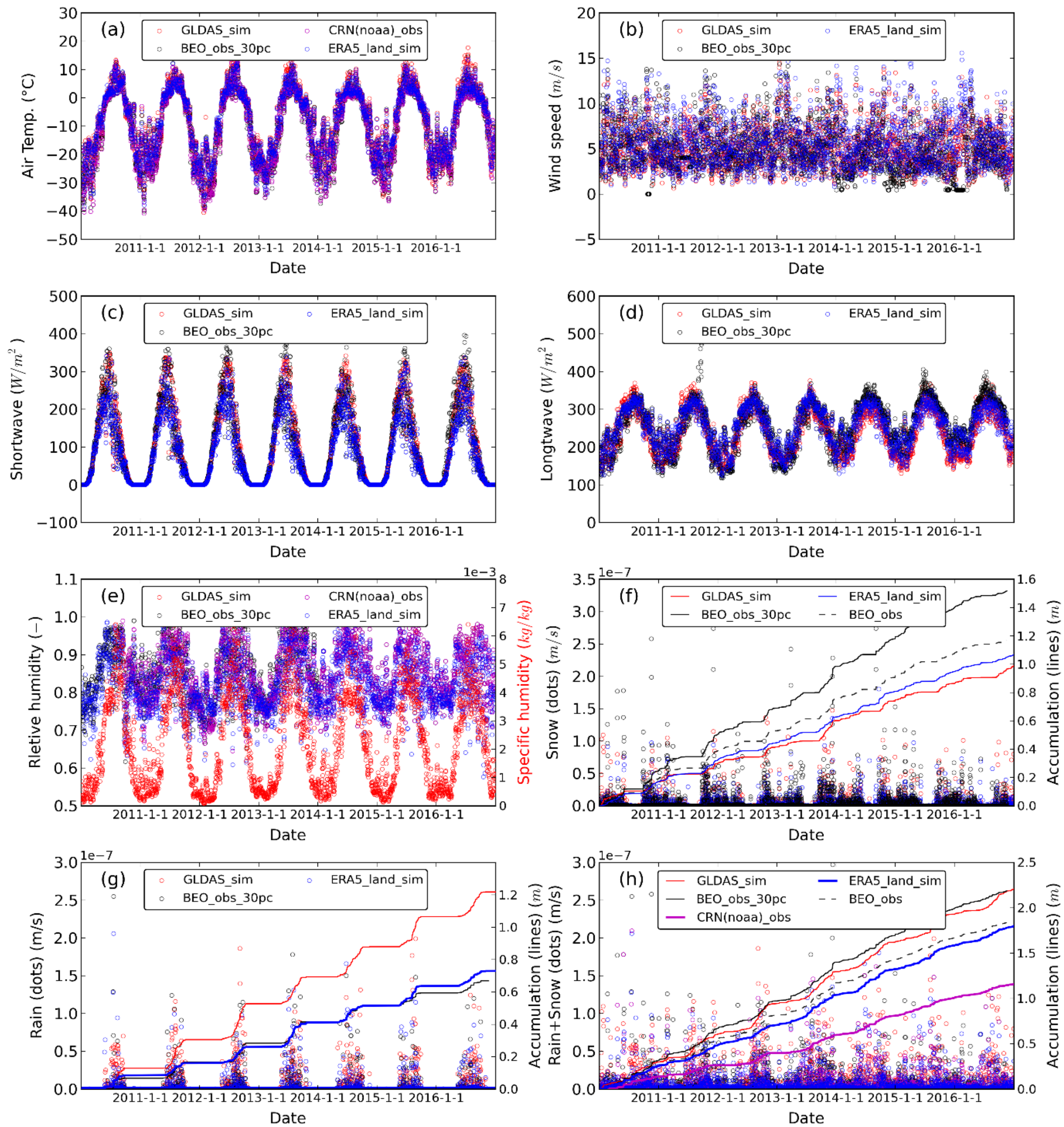

Figure S1. A graphical comparison of the meteorological forcing near Utqiagvik in Alaska (USA) was downloaded from four dataset sources for 2010-2016. The daily air temperature (a), wind speed (b), shortwave radiation (c), longwave radiation (d), relative humidity and specific humidity (e), snowfall rate and its accumulation depth (f), rainfall rate and its accumulation depth (g), total precipitation and its accumulation depth (h), were provided by the (1) re-analysis dataset ERA5-land (accessed: https://www.ecmwf.int/en/era5-land), (2) re-analysis dataset GLDAS (NASA) (accessed: https://disc.gsfc.nasa.gov/information/tools?title=Hydrology%20Data%20Rods), (3) observational dataset CRN (NOAA) (accessed: https://www.ncei.noaa.gov/access/crn/qcdatasets.html), and (4) observational dataset at the Barrow Environmental Observatory (BEO) (Atchley et al., 2015; Jan et al., 2020).

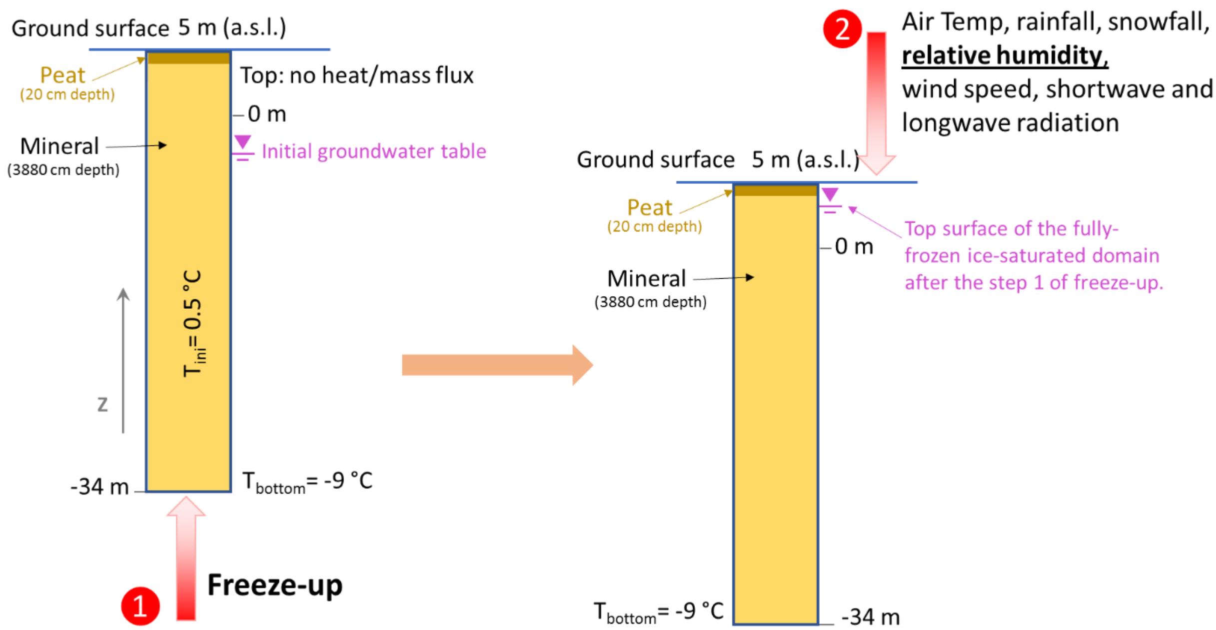

Figure S2. The 1D computational domain and model setup. Amanzi-ATS, an integrated hydrothermal process-based model, was used to study the impact of different formulations of SVP (saturation vapor pressure) and RH (relative humidity) on Arctic permafrost. The computational domain, boundary conditions, and parameters are tailored for a tundra site at Barrow, Alaska. The workflow includes two steps: i) bottom-up freezing of an initial unfrozen variably-saturated soil column to generate ice column at a steady state (with an upper region of the variably-saturated partially frozen status); ii) 13 different meteorological datasets from 2010 to 2016 were used to drive (top-down) the permafrost column model.

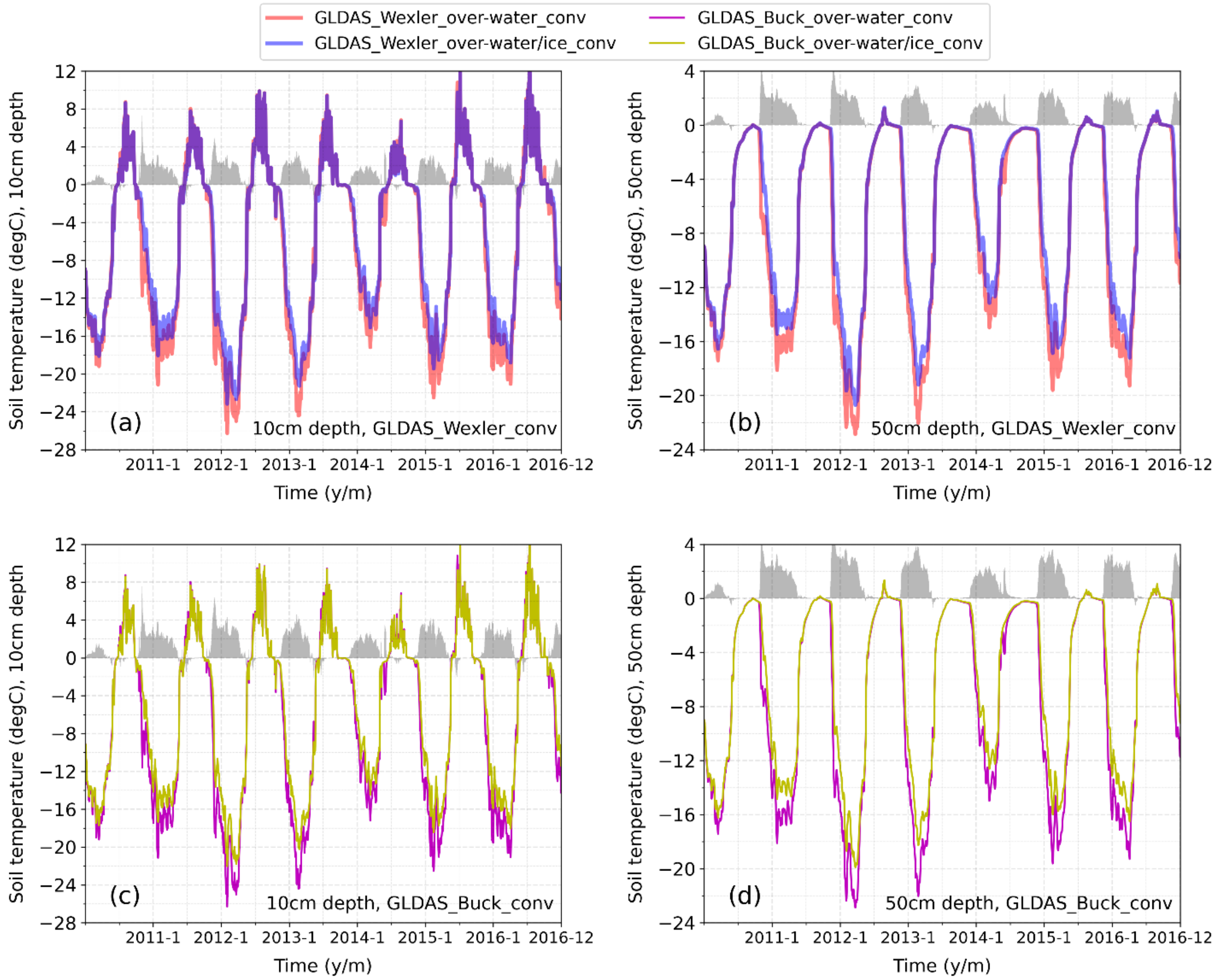

Figure S3. The simulated soil temperatures at a depth of 10 cm (a, c) and 50 cm (b, d) using the GLDAS dataset by converting the SHs to RHs based on the Wexler formula (a, b) and the Buck formula (c, d) over the years 2010-2016. The filled areas in grey denote the residuals between each formulation.

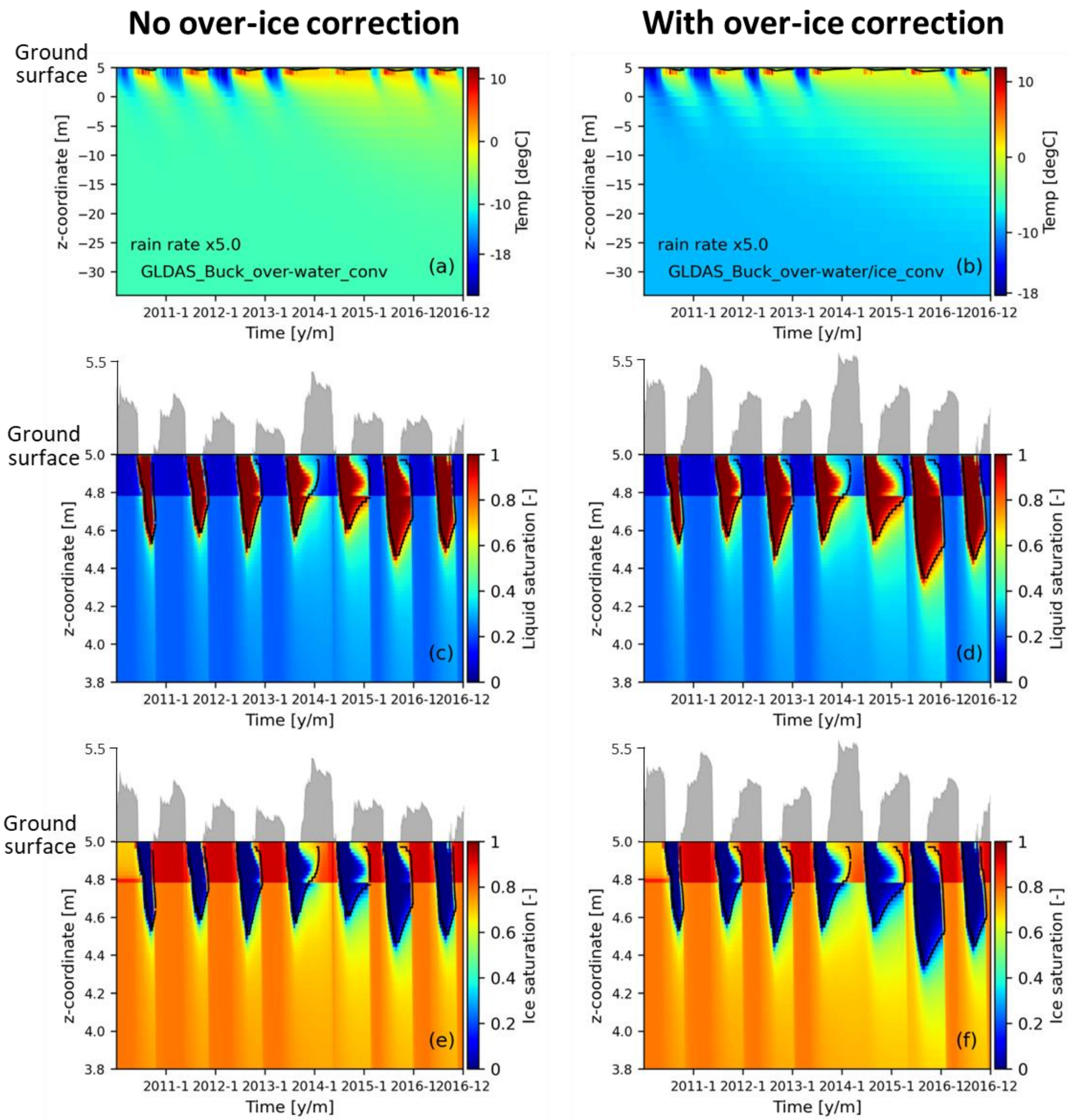

Figure S4. The evolution of the simulated ground temperature (a, b), saturation degree of the unfrozen liquid water (c, d), and saturation degree of the ice (e, f) using GLDAS dataset by converting the SHs (specific humidity) to RHs (relative humidity) based on Buck formula for calculating the SVP (saturation vapor pressure) without (left column) or with (right column) over-ice correction the years 2010-2016. The rain rate was increased five times (to mimic a heavy rainfall event), and the ponded water over the ground surface was limited to less than 1.0 m (the simulation settings are identical to those in Figure 3). The continuous black lines are the 0 °C isotherms in the ground, and the filled-up gray areas are the snowpack.

Table S1. The key subsurface physical properties used in the ATS model.

Parameter	Peat	Mineral
Porosity (-)	0.85	0.5
Intrinsic permeability (m^2)	5.0×10^{-11}	2.0×10^{-13}
Hydraulic conductivity ($m\cdot s^{-1}$)	5.51×10^{-4}	2.21×10^{-6}
Saturated water content ($m^3\cdot m^{-3}$)	0.85	0.5
Residual water content ($m^3\cdot m^{-3}$)	0.05	0.2
van Genuchten alpha α (Pa^{-1})	0.0005	$2x10^{-5}$
van Genuchten n (-)	1.39	1.58
Thermal conductivity, saturated unfrozen ($W\cdot m^{-1}\cdot K^{-1}$)	0.67	1.0
Thermal conductivity, dry ($W\cdot m^{-1}\cdot K^{-1}$)	0.07	0.29
Unsaturated alpha frozen (-)	1.0	1.0
Unsaturated alpha unfrozen (-)	0.5	0.5